



**HAL**  
open science

## Tactile discrimination of real and simulated isotropic textures by Friction-Induced Vibrations

Livia Felicetti, Chloé Sutter, E. Chatelet, Antoine Latour, Laurence Mouchnino, Francesco Massi

► **To cite this version:**

Livia Felicetti, Chloé Sutter, E. Chatelet, Antoine Latour, Laurence Mouchnino, et al.. Tactile discrimination of real and simulated isotropic textures by Friction-Induced Vibrations. *Tribology International*, 2023, 184, pp.108443. 10.1016/j.triboint.2023.108443 . hal-04059359

**HAL Id: hal-04059359**

**<https://cnrs.hal.science/hal-04059359>**

Submitted on 20 Jun 2023

**HAL** is a multi-disciplinary open access archive for the deposit and dissemination of scientific research documents, whether they are published or not. The documents may come from teaching and research institutions in France or abroad, or from public or private research centers.

L'archive ouverte pluridisciplinaire **HAL**, est destinée au dépôt et à la diffusion de documents scientifiques de niveau recherche, publiés ou non, émanant des établissements d'enseignement et de recherche français ou étrangers, des laboratoires publics ou privés.

# Tactile discrimination of real and simulated isotropic textures by Friction-Induced Vibrations

Livia Felicetti<sup>1-2)\*</sup>, Chloé Sutter<sup>3)</sup>, Eric Chatelet<sup>2)</sup>, Antoine Latour<sup>4)</sup>, Laurence Mouchnino<sup>3,5)</sup>, Francesco Massi<sup>1)</sup>

<sup>1)</sup> Department of Mechanical and Aerospace Engineering, Sapienza University of Rome, Rome, Italy

<sup>2)</sup> Univ. Lyon, INSA Lyon, CNRS, LAMCOS, UMR5259, 69621 Villeurbanne, France

<sup>3)</sup> Cognitive Neurosciences Laboratory, Aix-Marseille Univ., CNRS, Marseille, France

<sup>4)</sup> Univ. Grenoble Alpes, CEA LITEN, Avenue des Martyrs 17, 38000 Grenoble, France

<sup>5)</sup> Institut Universitaire de France, Paris, France

\*Corresponding author: livia.felicetti@uniroma1.it

## Abstract

Friction-induced vibrations are one of the main mechanical signals that, stimulating the mechanoreceptors, mediate the fine surface texture perception. In this work, isotropic textures are simulated by means of a tactile device reproducing the friction-induced vibrations previously measured during the exploration of real textures. Texture discrimination campaigns have been carried out, showing excellent results in discriminating both the real textures and the ones simulated by the device. Discrimination errors and correct associations of real and simulated samples have been explained through the spectra of the friction-induced vibrations, highlighting that the overall amplitude of the induced vibrations and their spectra play a fundamental role in the discrimination of isotropic textures.

**Keywords:** tactile perception, friction-induced vibrations, texture rendering, texture discrimination

## 1. Introduction

Our perception of the surrounding world is mediated by the five senses. Unlike the senses of sight and hearing, touch is an experiential process that requires contact and interaction with the object to be explored. The entire musculoskeletal system and the haptic system are involved in the tactile perception process, which is mediated by different types of mechanical stimuli: forces (stress distribution) and deformations (strain distribution), friction, vibrations (stress and strain transient oscillations), temperature, etc. Then, mechanical stimuli are detected by different types of receptors located in the skin, muscles, and tendons [1-2]. The detected stimuli are then transformed into electrical signals and sent to the brain, which interprets them.

To comprehend and to master touch stimuli, as we are able to do with visual and acoustic ones, it is necessary to investigate the main features of the mechanical signals that stimulate the mechanoreceptors. In this context, researchers are aiming to investigate the tactile perception mechanisms, and the relationships between the touched surface texture, the mechanical stimuli and their perception and discrimination [3-19].

According to recent studies, the vibrational signals are one of the main tactile stimuli, which mediate the discriminative perception of the fine textures [20-22]. When a surface texture is explored with the finger, Friction-Induced Vibrations (FIV) are generated at the contact interface [3-4,6-10,12-13,23-24,19]. The FIV signals show characteristic features depending on the surface texture topography and properties, the fingerprints topography, the contact boundary conditions (speed, contact loads, finger-surface angle etc.), and on the exploratory movements (proximal, distal, alternate, anteroposterior, lateral, circular etc.) as well [3,6,8,10,13,15,19,25-27].

Recently, key features of the FIV stimuli and friction forces have been investigated when exploring different kind of textures: textiles [11-12,23,28], periodic [3,6,13,29], isotropic [3] and common object's surfaces [4]. For example, FIV spectra associated to fabrics showed well-defined frequency peaks, linked to the period of the texture, and a broadband frequency content, linked to the isotropic component of the fibre hairiness [23]. In periodic surfaces, the main FIV frequency peak is strongly correlated with the sliding speed, the periodicity of the texture, and the fingerprints wavelength [10,13]. Moreover, in case of periodic textured topographies, strong correlations between the FIV frequency distribution and the descriptive and hedonistic perception of the surfaces were found [3,5-11,13,17,29].

Overall, these recent studies, highlighting the main role played by the FIV in the fine texture discrimination, paved the way to the possibility to artificially simulating the tactile perception by reproducing the "texture vibrations".

Tactile rendering of textures is a ground-breaking social and technological challenge. The applications of such a technology may be promising, in all the everyday field of the human life, e.g., in medical field, remote surgery and tele-operations, virtual and augmented reality, human-machine interfaces, in biomedical engineering, for detection and rehabilitation of tactile deficiencies, in e-commerce enabling to perceive the texture of an object, through a tactile device and/or screen...

Currently, different tactile devices, based on different working physical principles and dealing with different mechanical tactile stimuli, can be found in literature [30-34]. The most used tactile rendering approaches are the vibrotactile [35-37], the electrostatic [38-42] and the ultrasonic [28,43-45] ones. Some efforts are being made to combine these different rendering approaches [46-47]. Electrostatic and ultrasonic tactile screens are based on friction modulation at the contact between the user's fingertip and the device, that is achieved, respectively, by the generation of electrostatic forces and by an air film caused by the ultrasonic actuation. The vibrotactile rendering is already used to recreate some simple haptics effects or feedbacks, for example in mobile phones and videogame controllers. Some recent studies begin to explore the possibility to render fine textures via vibrotactile devices [35-37,48-50].

For the three rendering modalities (vibrotactile, electrostatic, ultrasonic), a data-driven approach is often used: mechanical signals are acquired from real surface textures to be subsequently reproduced by the device [28,35-36,39,41-43,47-50]. Databases of mechanical signals, such as acceleration, velocity and friction forces, measured during real texture exploration can be found in literature [51-53]. In most of the cases, in the data-driven vibrotactile rendering, the measured mechanical signals by the surface exploration are obtained by a stylus or a rigid tool [35-36,47-50]. This can be considered as a limitation in the simulating approaches, which ignore the primary role of the skin, and therefore the fingerprints, in the generation of the FIV at the contact interface. This fundamental aspect is taken into account in the present work, by measuring and analysing the FIV obtained by the participants' fingertip directly scanning the surface and by considering the finger's transfer function in the rendering signal process.

The present work, belonging to the data-driven vibrotactile approach, exploits a novel Electro-Active Polymer (EAP) piezoelectric actuator technology, which has interesting technological characteristics: lightness, small thickness, flexibility, a certain degree of transparency, and the possibility to be realized in many geometries and dimensions (printed on flexible support) [54-58]. Those characteristics make it suitable to be employed in wearable tactile devices, such as, for example, tactile gloves.

The discrimination of randomly textured surfaces is here approached by investigating and mimicking the mechanical stimuli, particularly the FIV. The FIV stimuli associated to the finger sliding on isotropic surfaces have been measured and analysed to better comprehend the key features of the obtained signals. Then, the tactile device, named PIEZOTACT, has been employed to reproduce the measured FIV stimuli and simulating the surface tactile perception. Discrimination campaigns (by a panel of volunteers) on real and simulated textures are then possible, allowing for investigating the role of the FIV spectra on the texture discrimination.

## 2. Materials and method

### 2.1. Overall approach

In the first instance, the manufacturing process to obtain the isotropic samples to induce the tactile stimuli is presented. Then, the test benches used to measure and investigate the mechanical stimuli, associated to the exploration of the isotropic samples by both active and passive touch, will be discussed. While active touch is used for discrimination campaigns, passive touch measurements are necessary to compare the measured signals in controlled boundary conditions. Then, the developed tactile rendering device, named PIEZOTACT [9], which allows to reproduce, by means of an actuator, the previously measured FIV signals, is exploited for mimicking tactile stimuli obtained by active touch of textures. Finally, a discrimination campaign, performed with 10 volunteers, is performed to verify the possibility to discriminate the rendered textures using the PIEZOTACT device and whether it is comparable to the real isotropic texture discrimination. The results of the discrimination campaign are then discussed, and the errors and correct discriminations of the touched samples will be explained by the main features of the FIV spectra.

### 2.2. Surface samples

The used surfaces as tactile stimuli are constituted of 14 isotropic samples with randomly rough topography [17]. The samples are made of bicomponent epoxy resin (Prochima E-30). The set of samples (Fig. 1a) is constituted of 13 surfaces obtained by silicone moulding and resin casting of glasspaper of different grain sizes (from P40 to P4000), plus a sample obtained by the free surface of the epoxy resin (this sample has been denominated as 'no texture', although it has its own texture, i.e. the epoxy resin crystal surface topography. Referred as "NO" in the following graphics and tables). The used procedure and materials to produce the 14 samples is explained in the following:

- In the first instance, a mould matrix has been produced by additive manufacturing (3D printing of PLA). The mould matrix was the support on which each square of glasspaper, of edge 50 mm, was glued (Fig. 1b).
- Then, the bi-component silicone (ELKEM BLUESIL RTV 3428) was poured in a container and the mould matrix was immersed into the silicone (Fig. 1c). Once the silicone solidified, the matrix was extracted (Fig. 1d).

- At this point, the epoxy resin was poured into the obtained silicone mould. Once the resin was solidified, it was extracted, and squares having side of 50 mm and thickness of 4 mm were obtained (Fig. 1e).
- Then, the samples were observed at the numerical microscope KEYENCE WHX 2000 to recover their topographical features (Fig. 2). Table 1 reports the roughness Ra of the used samples, as well as the corresponding original glasspaper grade. For this study, it was chosen to sort the sequence of samples according to the measured roughness, in term of Ra. Because S7 and S8 samples (corresponding to P400 and P600 glasspapers) were found to have the same measured Ra, it was decided to order them according to the original glasspaper grade. The only inversion found, with respect to the original glasspaper grade, was between samples P1000 and P4000 (corresponding to samples S10 and S13).

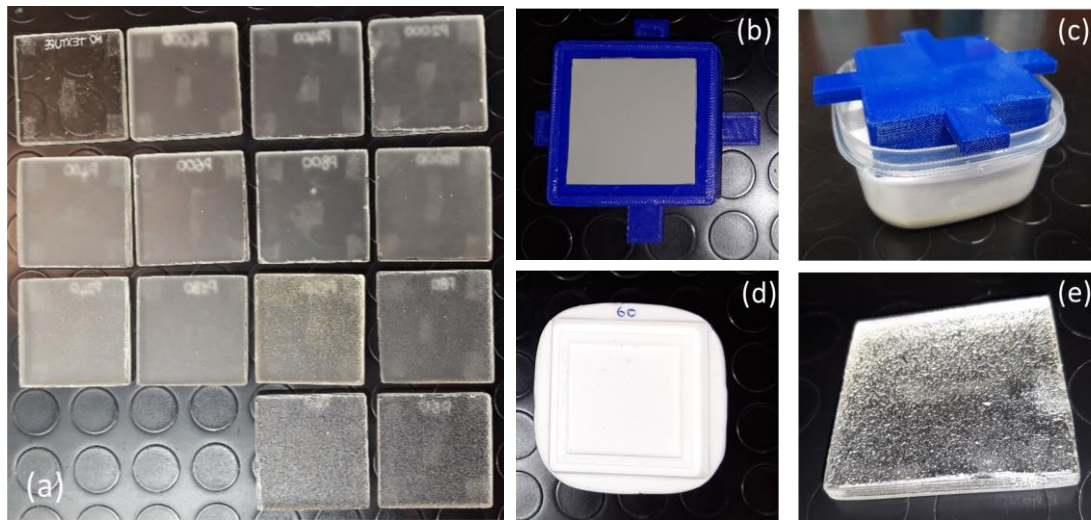


Figure 1: Manufacturing of isotropic samples: (a) the 14 isotropic epoxy resin surface samples; (b) mould matrix with the glasspaper glued on it; (c) mould matrix into the silicone; (d) obtained silicone mould; (e) obtained sample in epoxy resin.

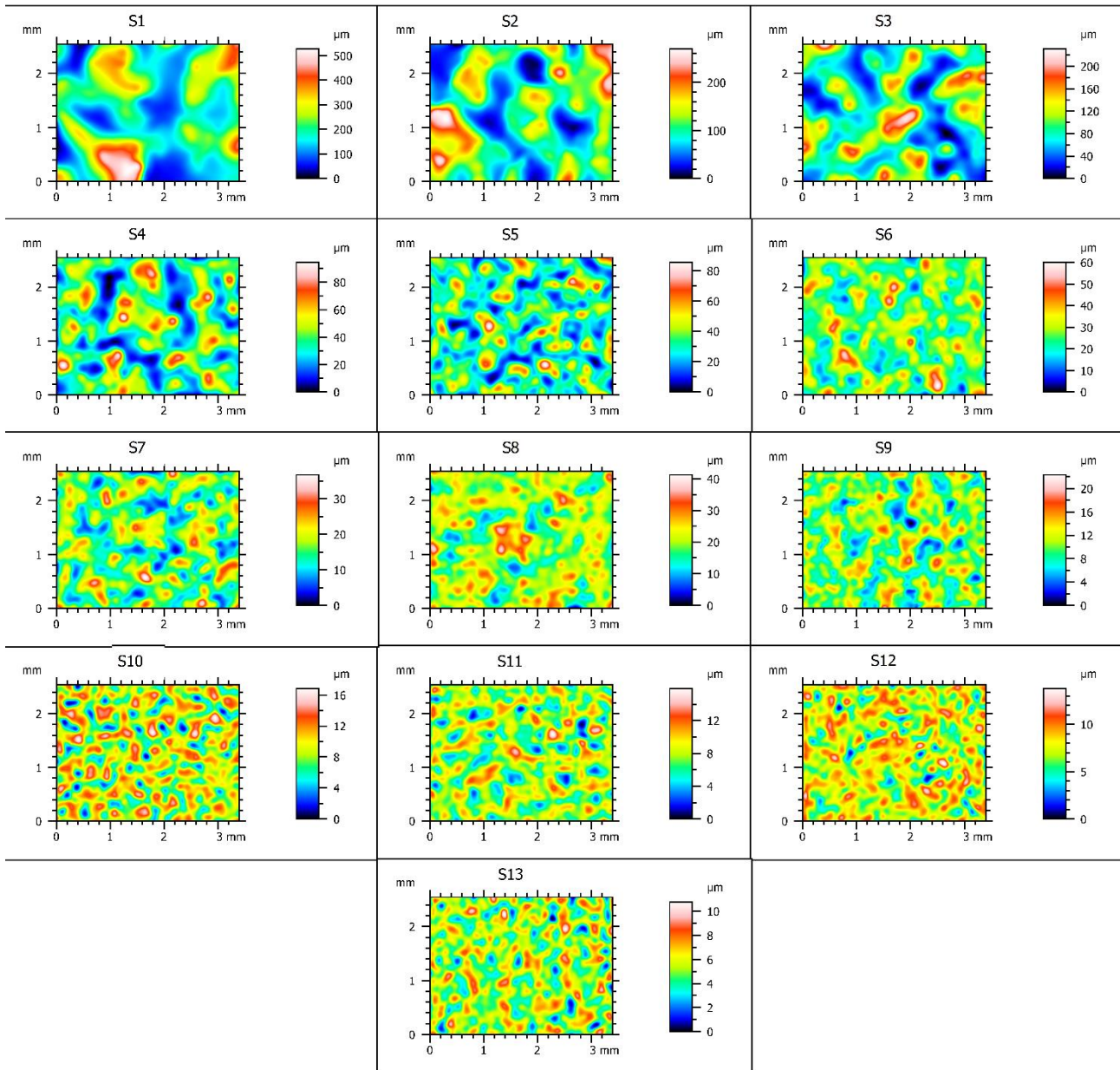


Figure 2: Isotropic sample topographies (VHX Keyence).

Table 1: Isotropic sample roughness (Ra) and original glasspaper grade.

| Sample | # glasspaper | Ra [ $\mu\text{m}$ ] |
|--------|--------------|----------------------|
| S1     | P40          | 74.6                 |
| S2     | P60          | 43.7                 |
| S3     | P80          | 33.6                 |
| S4     | P120         | 14.4                 |
| S5     | P180         | 11.7                 |
| S6     | P240         | 6.6                  |
| S7     | P400         | 5.2                  |
| S8     | P600         | 5.2                  |
| S9     | P800         | 4.6                  |
| S10    | P4000        | 4.5                  |
| S11    | P2000        | 4.4                  |
| S12    | P2400        | 4.3                  |
| S13    | P1000        | 3.8                  |
| NO     | /            | 0.1                  |

### 2.3. Test bench for passive touch measurements

In passive touch, the finger is kept motionless, and the surface sample slides under the finger, driven by an external mechanical system. This kind of tests allow to perform measurements with controlled boundary conditions; in particular, it is possible to control the sample sliding speed, in order to perform tests with a constant relative velocity between fingertip and surface.

To investigate the FIV, the contact forces and the friction coefficient (induced by the finger/surface interaction) under controlled operating conditions, a specific linear tribometer, the TriboAir test bench, is used (Fig. 3). Since the FIV induced by the finger/surface interaction are generally characterised by low amplitudes, it is important to prevent parasitic vibration and noise coming from the mechanical system and the contact interfaces. The TriboAir test bench allows to avoid parasitic vibrations thanks to the design of the moving platform, driven by four air bearings, moving along two shafts, and a voice coil actuator. Thus, the platform is completely suspended on air, and the only contact originating FIV is the one under investigation. The controlled sliding motion is ensured by a linear voice coil motor (BEI KIMCO LA30-75-001A) and a linear optical encoder (MicroE OPS-200-1-1), which allow to define the law of motion and the platform sliding velocity thanks to a PID controller (ELMO Gold DC Whistle, G-DCWHI10/100EE). The contact forces are measured by two tri-axial force transducers (KISTLER 9017C) mounted on the platform. More details on the TriboAir test bench can be found in [59-60].

In order to perform the passive touch measurements, the participant places the finger on the surface sample, fixed on the top of the sliding platform. The normal contact force between finger and surface, which can be monitored during the test, is imposed directly by the participant. The arm is placed on a support to maintain a constant finger/surface inclination (about 15-20 degrees), and to help the participant to keep the finger stationary and the normal force constant. Before the platform motion starts, the participant place the finger on the surface sample. Since the finger is motionless and the TriboAir platform slides in distal direction with respect to the finger, the relative velocity of the finger with respect to the surface sample results to be in proximal direction. The participant is asked to maintain a constant normal load of approximately 0.2 N (the subject can see the recorded normal load on the laptop monitor). Then, after the surface sliding motion ends,

the participant lifts the finger. The same test is repeated at least 6 times for each surface. The FIV (acceleration) signal is acquired by an accelerometer (PCB 352A24, PCB Piezotronics, Inc.) glued by wax on the fingernail of the subject. The acquired data, at a sampling frequency of 5kHz, are then exported to Matlab to perform the desired signal post-processing. Frequencies up to 10Hz have been filtered to eliminate involuntary hand movements. This filter does not affect the results, especially in terms of analysis and mimicking of FIV stimuli, because they fall in a frequency range that is at the limit of the mechanoreceptor reception frequency field. Although the acquisition frequency of the signals is 5kHz, in the following, the figures will be presented in a range of frequencies up to 1kHz, the frequency range of interest for tactile perception, to facilitate the readability of the graphs, as no significant spectral content has been detected beyond 1kHz (with the only exception of Figure 13).

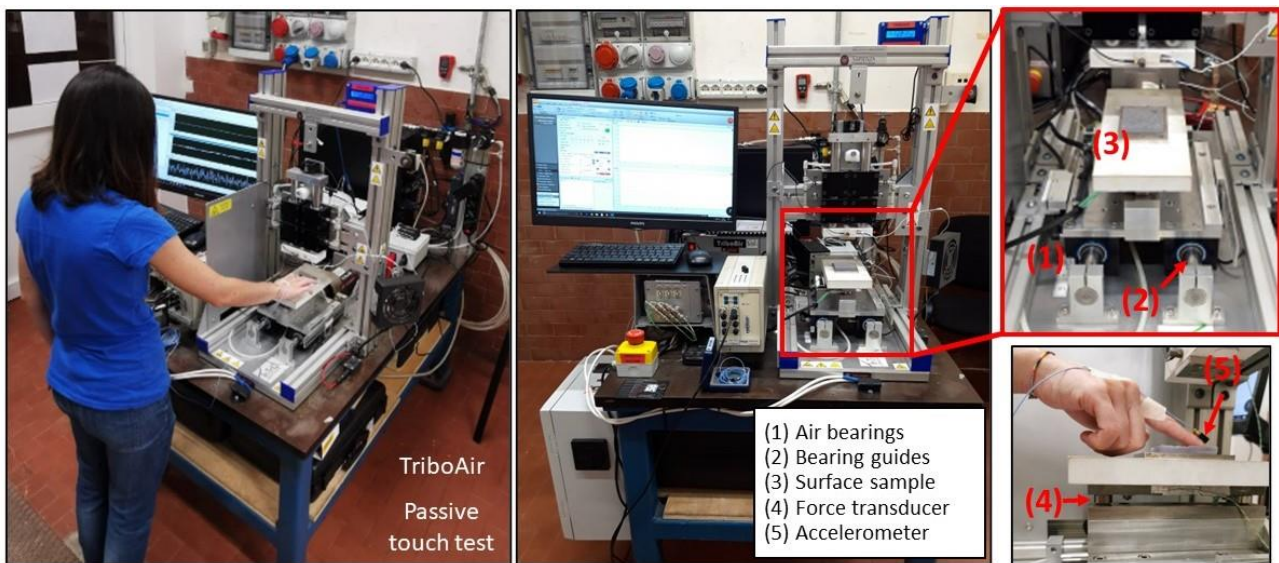


Figure 3: TriboAir test bench for passive touch tests. The surface sample is fixed on the moving platform, driven by air bearings to avoid parasitic vibrations. During the platform motion, the participant's finger is on the surface sample. An accelerometer on the fingernail recovers the acceleration signal, while two tri-axial force transducers measure the contact forces.

## 2.4. Test bench for active touch measurements

Active touch of a surface is the effective mode used to explore the surface textures [9,17]. To perform the active touch tests, the participant strokes the finger on the surface sample, while the surface sample is kept motionless. The boundary conditions, such as sliding velocity, contact forces and finger/surface angle are imposed by the participant. To recover the contact forces, the surface sample is fixed with double sided tape on the top of a triaxial force transducer (Testwell K3D60). For the present analysis, the finger motion is in proximal direction (sliding velocity parallel to the finger axis). The participant strokes the index finger of the dominant hand on the surface samples 10 times, lifting the finger between strokes. Because the real active exploration of a surface does not take place only in the proximal direction, the sliding motion used in this work represents an "ideal" condition of active touch. Based on previous experiences and literature, a proximal (non-alternate) exploration movement was chosen in order to maximize vibratory signals and to reduce the occurrence of stick-slip phenomena [15,19,26]. An accelerometer (PCB 352A24, PCB Piezotronics, Inc.) is fixed by wax on the fingernail of the participant to measure the FIV (acceleration) signal originated by the sliding of the finger on the surface sample. The contact forces and acceleration signals are acquired by a SIRIUSi (DeweSoft) acquisition system (based on DualCoreADC® technology with dual 24-bit delta-sigma

analog to digital converter) at a sampling rate of 5kHz. The boundary conditions are imposed by the participant, who is asked to maintain a normal contact load approximately around 0.2 N and a finger/surface inclination of approximately 15-20 degrees. Within the range of normal forces identified in literature [61], preliminary tests of active touch allowed to identify an average force of about 0.2 N, used by the participants to naturally explore the tested surfaces. Moreover, the participant is asked to maintain, with the aid of a metronome, approximately the same exploration time during all the tests on all the tested surface samples. Although it is an active touch, this protocol makes possible to perform tests with semi-controlled boundary conditions. The acquired data, with DeweSoft software, are then exported in Matlab to be post-processed and to analyse the measured signals. Figure 4 shows the active touch experimental setup.



Figure 4: Active touch setup for measurement of contact forces and acceleration (FIV) during active exploration of the surface samples.

## 2.5. PIEZOTACT device to mimic the tactile FIV stimuli

A tactile device, named PIEZOTACT, based on an Electro-Active Polymer (EAP) piezoelectric actuator, is used to reproduce the tactile FIV stimuli measured when touching surface textures [9,17]. The EAP piezoelectric actuator is fixed into a PLA support produced by additive manufacturing. The actuator driving chain is constituted by a PC and an electronic card (Texas Instruments DRV2667EVM-CT). The PIEZOTACT device is represented in Figure 5. The methodology at the basis of the PIEZOTACT device exploits the transfer function of the device, including the finger of the experimenter, the actuator, and the electronics of the device, to pre-process the FIV (acceleration) previously measured by sliding the finger on the real surfaces. The following steps have been then performed for the FIV mimicking:

- The transfer function is preliminarily characterized by sending a random signal as input by the Matlab software to the PIEZOTACT device, and by measuring the output acceleration signal thanks to an accelerometer fixed on the fingernail, with the finger placed in static contact with the actuator surface;
- then, in order to reproduce the FIV signals obtained from the real surface, the Fast Fourier Transform (FFT) of the FIV signal, measured with the active touch protocol described in section 2.4 on the isotropic surface sample, is divided by the previously obtained transfer function;

- the Inverse Fast Fourier Transform (IFFT) is calculated to be the input of the device, ensuring the correct FIV reproduction by the device on the fingertip;
- the obtained time vector is finally sent by the PC as an audio signal to the Texas Instruments (TI) card to drive the actuator.

The development, the mimicking protocol, and validation of the tactile PIEZOTACT device are described in detail in [9]. Figure 5 shows the experimental setup: the PC (3) is used as signal generator to send the pre-processed FIV signal (audio signal) to the TI card (2), to drive the EAP actuator (1); the actuator, fixed into the PLA support, is fixed on a tri-axial force transducer (5); an accelerometer (6) is fixed on the fingernail of the experimenter, who keeps the finger on the actuator surface; then, the signals measured by the accelerometer and the force transducer are sent to the acquisition system (4) (SIRIUSi – DEWESOFT) and acquired by the DeweSoft software.

In order to validate the mimicking protocol, the original FIV (acceleration) signal, measured during the active touch of the real surface sample, can be compared with the one acquired by the accelerometer on the fingernail during the reproduction of the vibrational signal by the rendering device (reproduced/simulated surface), as explained in [9]. An example of comparison, between the FIV measured when exploring an isotropic surface and the corresponding one simulated by the PIEZOTACT, is reported in Figure 6a. The green curve represents the spectrum of the original signal measured during the exploration of the real isotropic texture, while the black curve is the spectrum of the recovered signal when touching the actuator surface, vibrating with the mimicked FIV. In both cases, the acceleration is measured by the accelerometer fixed by wax on the fingernail of the participant, as can be seen in Figure 6b and 6c. The good agreement between the two spectra testifies the reliability of the approach. Moreover, being the finger transfer function the same for the two cases, the stimulation at the mechanoreceptors in the fingertip will be, with a good approximation, similar, when touching the real and simulated texture.

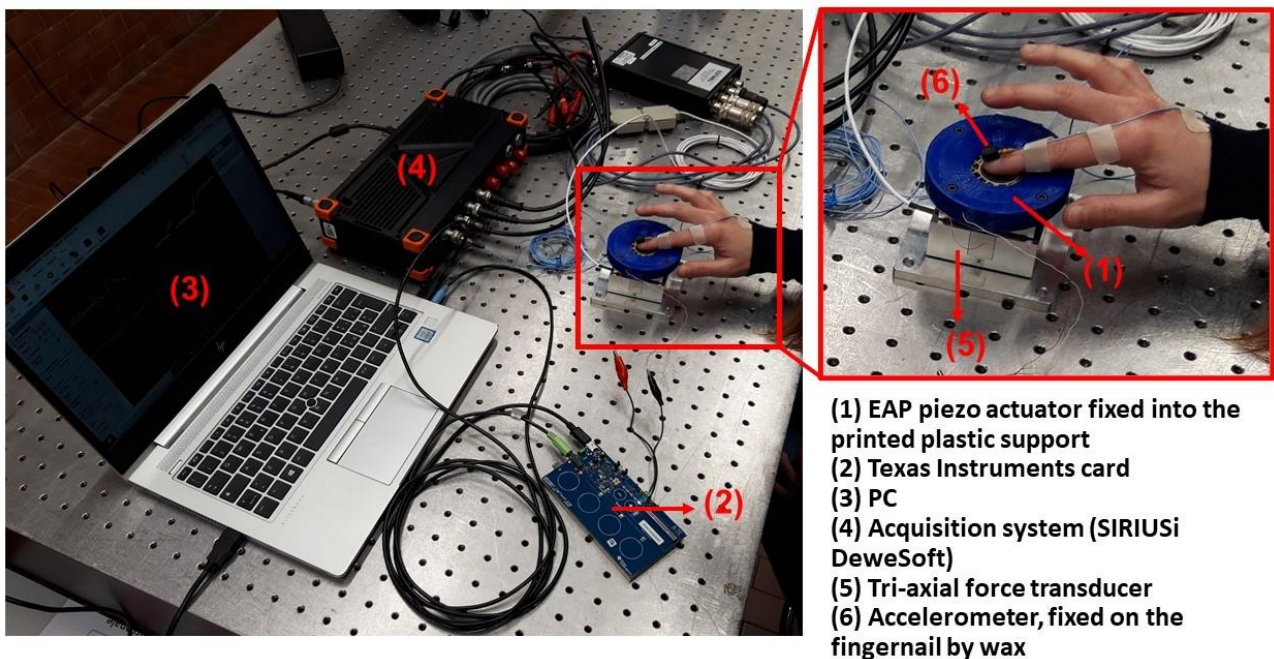


Figure 5: The PIEZOTACT tactile device with the experimenter's finger, during the verification of the correct signal reproduction. The pre-processed signal is given as input from Matlab to the device. The output acceleration is measured by the accelerometer on the fingernail. The same experimental setup is used to measure the device and finger transfer function. In this case, a random signal up to 1000 Hz is sent as input from Matlab to the device.

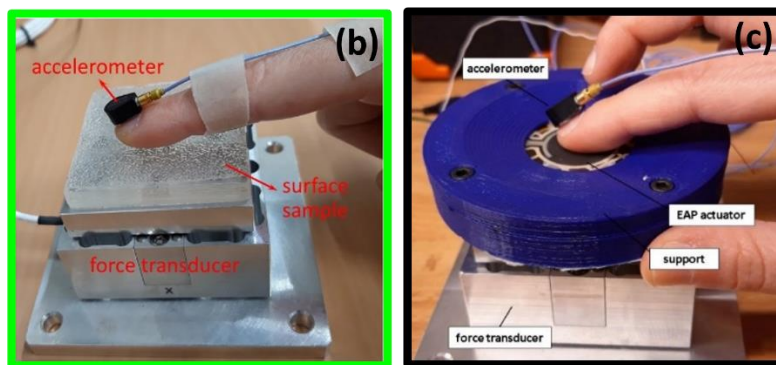
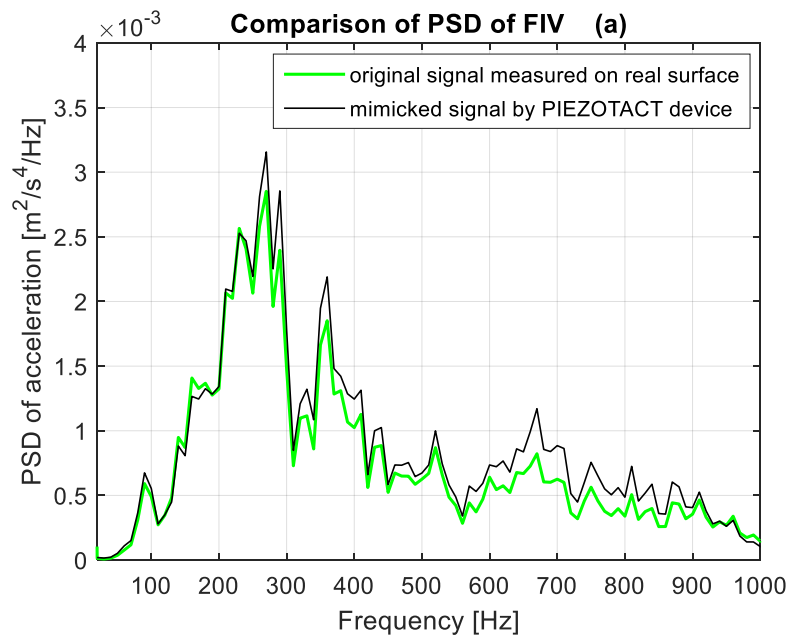


Figure 6: (a) comparison between the FIV measured on a real isotropic sample (green curve) the corresponding mimicked signal by the PIEZOTACT device (black curve); (b) used setup to measure the FIV by exploration of the real texture; (c) used setup to recover the acceleration when the finger is in contact with the vibrating actuator.

## 2.6. Discrimination campaign protocol

A discrimination campaign on a panel of 10 participants (1 female and 9 males, with age ranging between 21 and 44 years, 1 lefthander and 9 righthanders) has been carried out for both the real and the simulated (reproduced FIV by the PIEZOTACT device) textures. The aim is to investigate the correlation between the mechanical stimuli, and particularly the FIV, and the capability of the participants to discriminate between the different isotropic randomly rough surfaces. Informed consent for experimentation was obtained by all the 10 involved participants and the privacy rights of human participants has been observed.

For each participant, the test was split into two sessions:

- During the first session (duration of approximately one hour), measurements of FIV and contact forces, according to the active touch protocol described in section 2.4, have been performed for each of the 14 surfaces. The transfer function of the PIEZOTACT device with the finger of the participant has been experimentally characterized as well, according to the protocol described in section 2.5.
- Before moving on to the second session, i.e. the discrimination tests, the obtained signals have been analysed and post-processed by the experimenter to be reproduced by the PIEZOTACT device, according to the methodology described in section 2.5 and reported in [9].

- For the second session (duration of approximately one hour and a half), the participant was instructed for the discrimination campaign on real and simulated surfaces. The discrimination campaign consisted into 3 different tasks.

The measurement session and the discrimination session did not take place on the same day, in order to avoid fatigue for the participants and to process the acquired data and obtain the signals needed to simulate the textures using the PIEZOTACT device. The participant underwent first the measurement session and was then recalled to carry out the discrimination session.

### TASK 1

The first task consisted into a preliminary test performed on all the 14 surface samples (Fig. 7). The samples were presented in a random order to the participant. The participant was blindfolded with scratched spectacles, allowing to distinguish the shape and position of the sample surfaces but not the texture. Before starting the test, the participant was asked to wash their hands with soap and water and then let them dry. It was then asked to the participant to touch and explore the 14 samples and to put them in order, from the roughest to the smoothest. No constraints concerning the used exploration procedure were imposed on the subject. No time limit was imposed to the participant to perform the task. This preliminary task allowed to investigate if the participant put the 14 samples in the corresponding order of the physical surface roughness; moreover, the participant could acquire familiarity with the tactile perception of the 14 surfaces. The task was repeated 3 times and the declared sequences by the participant were annotated by the experimenter.

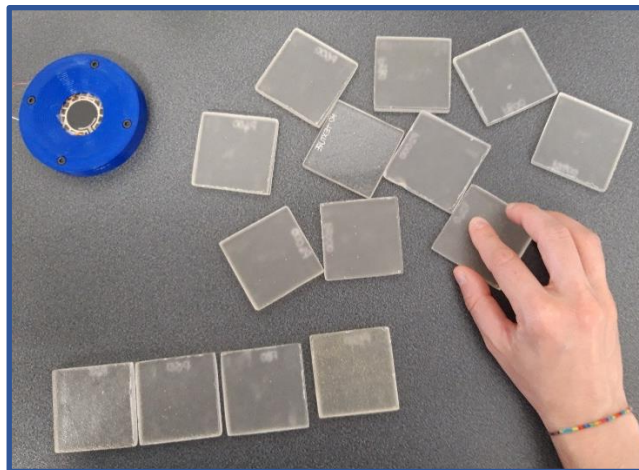


*Figure 7: In TASK 1 the participant put the 14 surface samples in order from the roughest one to the smoothest one.*

Then, to perform the second and third task, the surface samples have been randomly divided into groups, each constituted by 3 samples. The "no texture" sample has been excluded from the second and third tasks. In fact, being very smooth, the "no texture" sample gave rise to adhesion and stick-slip phenomena during the measurement phase, which resulted in high amplitude vibrations that could generate confusion for the participants. The used subsets of samples are reported in Table 2.

After performing Task 1, for each subset (triplet) of samples, the second and the third task have been consecutively performed. More specifically, for each subset of samples, the participant performed Task 2 and immediately after performed Task 3. Afterward, the next subset of samples was presented to the participant. This protocol was performed consecutively for all subsets of samples in Table 2.

Table 2: Used subsets of samples for the discrimination campaign on real (task 2) and simulated (task 3) surfaces.

| SET | SAMPLES |     |     |
|-----|---------|-----|-----|
| A   | S2      | S4  | S8  |
| B   | S5      | S7  | S9  |
| C   | S6      | S11 | S10 |
| D   | S1      | S3  | S13 |
| E   | S5      | S8  | S12 |
| F   | S5      | S9  | S10 |
| G   | S2      | S3  | S4  |
| H   | S1      | S8  | S13 |
| I   | S1      | S7  | S12 |
| L   | S4      | S13 | S10 |
| M   | S4      | S8  | S9  |
| N   | S13     | S12 | S10 |

## TASK 2

The second task consisted into a discrimination of real surface samples. The participant was blindfolded with scratched spectacles, which allow to see the shape and position of the 3 tested samples but prevent the participant to see the surface textures. Before starting the test, the participant was asked to wash his hands with soap and water and then let them dry. The 3 surfaces belonging to the tested set were then presented to the participant in a random order. The participant was then asked to touch and freely explore the 3 surfaces, and then to put them in order, from the roughest to the smoothest, entrusting only with the tactile sense. The subject was suggested to explore the real surfaces with the index finger of the dominant hand in a proximal direction, in conditions similar to those used for measuring FIV. No time limit was imposed to the participant to perform the task. Then, an identifier A, B, C was assigned to the samples, which were left in the order chosen by the participant for the next task (Fig. 8a). The declared sequence by the participant was annotated as well by the experimenter.

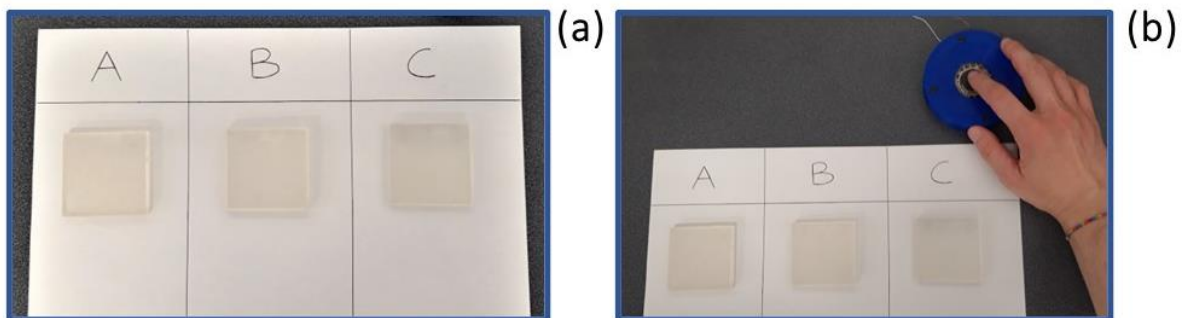


Figure 8: Task 2 (a) and task 3 (b), performed for each subset of 3 samples.

## TASK 3

The third task consisted into the discrimination of the simulated textures, thanks to the vibrational signal (FIV) mimicked by the PIEZOTACT device. For each set of samples, a random sequence of 3 or 4 simulated textures (reproduced FIV by the PIEZOTACT), chosen between the surfaces belonging to the same set

previously tested in Task 2, has been proposed to the participant. In the sequence there could be repetitions of the same signal, or a signal could be absent from the sequence. This prevented the participant to answer by exclusion. It was asked to the participant to perceive the sequence of signals by touching the vibrating actuator, and then to associate the reproduced signal to the corresponding real surface (A, B, C) (Fig. 8b). The participant was allowed to perceive a reproduced signal, or the entire sequence, more than once and to touch the real samples to compare the real and simulated surfaces. The participant wore earmuffs to avoid acoustic feedback from the actuator. No time limit was imposed to the participant to perform the task. The declared sequence by the participant was then annotated by the experimenter.

Finally, after comparing the outcomes of the different tasks between them, and with the surface roughness, the results have been analysed and discussed with regards to the FIV spectra characteristics.

## 3. Results and discussion

### 3.1. FIV by active touch

The FIV (acceleration) signals, obtained during active tactile exploration of the 14 isotropic samples, have been measured by the protocol presented in section 2.4. The average Power Spectral Density (PSD), associated to 10 active touch measures (i.e. 10 strokes of the participant finger) on each isotropic sample, have been then computed by the MATLAB software.

The measurements have been performed for each participant (with his/her own finger's characteristics) involved in the discrimination campaign, in order to obtain the FIV signals to be mimicked by the PIEZOTACT device.

The PSD spectra associated to the active touch of the 14 isotropic samples, by a representative participant taken as a reference, are presented in Figure 9. The isotropic samples show an overall large band spectrum, within the frequency range of mechanoreceptor main sensitivity (10-600 Hz). Qualitatively, the FIV associated to the 14 tested samples show a very similar large band frequency distribution. Coarser textures show a relatively large frequency peak corresponding to the fingerprints width, as expected by the literature [8,13,23]. Nevertheless, what varies the most between samples is the FIV amplitude, that goes from higher FIV amplitudes for coarser textures (higher roughness) to lower FIV amplitudes for smoother samples (lower roughness). The same qualitative trend has been recovered for all the 10 participants. This qualitative trend suggests that, when considering isotropic textures, the most important feature of the FIV spectra, distinguishing one texture from another, is the amplitude of vibration rather than the frequency distribution.

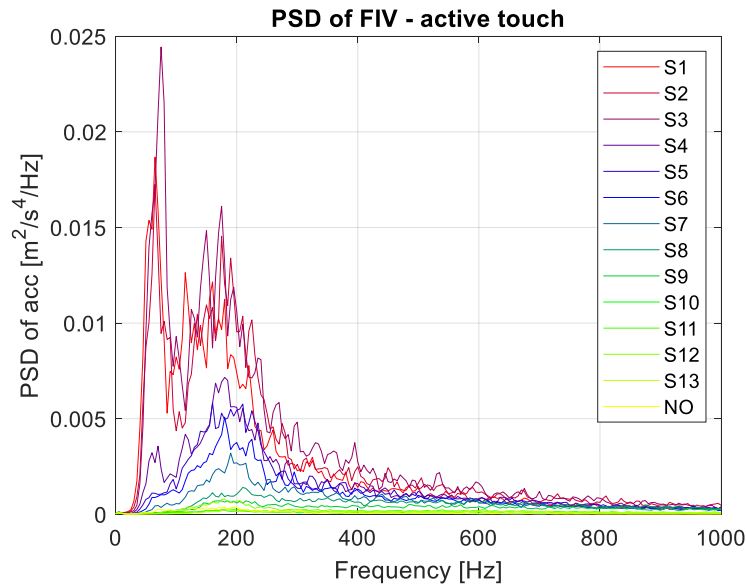


Figure 9: Comparison between the PSD spectra associated to the active touch of the 14 isotropic samples for a participant.

## 3.2. FIV by passive touch

A test campaign with controlled contact parameters has been carried out on a reference participant, in order to investigate the FIV spectrum when the contact velocity and load are controlled (passive touch). To perform FIV measurements by the finger/surface interaction in controlled conditions, the TriboAir test bench and the protocol described in section 2.3 have been used.

Figure 10 shows the average FIV spectra associated to the 14 isotropic samples, measured for the reference participant, with a constant sliding velocity of 30 mm/s, imposed by the test bench. The analysis of the PSD, obtained with controlled sliding velocity, confirms the trend found in active touch (Fig. 9). The 14 samples present large band spectra, with a similar FIV frequency distribution, and a variation in the FIV amplitude is recovered between samples. As well, the general qualitative trend shows that higher FIV amplitudes are associated to coarser textures (higher roughness), while lower FIV amplitudes are obtained for smoother samples (lower roughness).

When comparing the trend for the tested isotropic randomly rough surfaces with the results of a previous study [13], related to periodic textures, different key features can be highlighted.

In periodic textures, the frequency distribution of the induced vibrations was correlated to the clustering of the surfaces in by different perceptual descriptors, such as “rough” or “adhesive”, “textured” and “smooth” [13]. The periodic textures showed clearly different FIV frequency distributions, with well-defined peaks in frequency, which could be associated with the “descriptive” and “hedonistic” perception of the textures. The FIV amplitude played a role only in the perception of the coarser periodic textures, for which the FIV had a similar frequency distribution, and the surfaces were clustered, on the basis of the FIV amplitude, in “rough” or “adhesive”. Thus, for the periodic textures, finer textures were well clustered by the frequency distribution, while the amplitude of the induced vibrations played a role in discriminating the coarser textures. More detailed information on the referred previous study on periodic surfaces can be found in [13].

The isotropic textures, object of this work, show FIV spectra characterized by a similar wide frequency band, with no significant differences in the frequency distribution between samples, independently from the roughness associated to each sample. On the contrary, the vibration amplitude varies significantly between the 14 samples, quite consistently with the trend of the sample roughness. Therefore, for isotropic random

textures, the most important FIV feature, distinguishing between the surface samples, seems to be the amplitude of the induced vibrations.

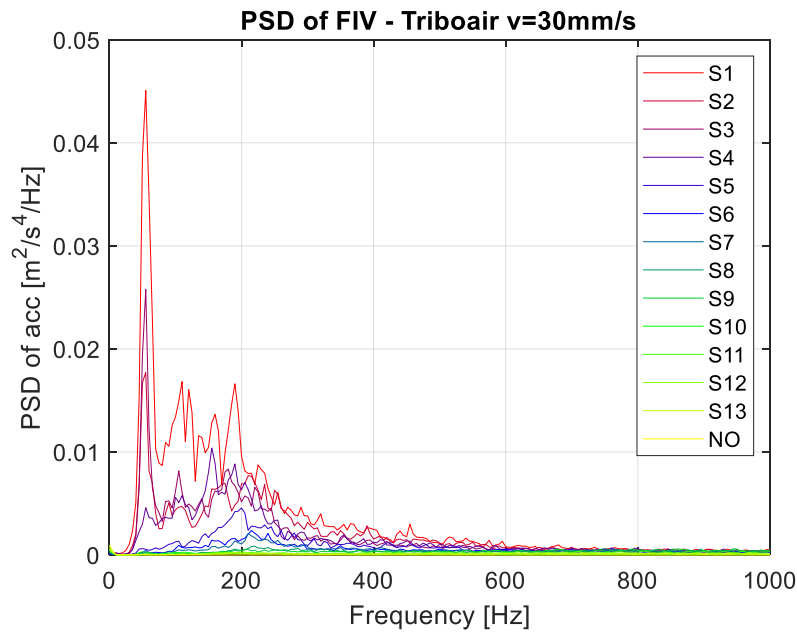


Figure 10: Comparison between the PSD spectra associated to the passive touch of the 14 isotropic samples for a participant.

### 3.3. Active touch vs passive touch

The FIV spectra obtained by active and passive touch (Fig. 9 and 10), when exploring isotropic samples, show a similar overall trend with respect to the surface roughness. The spectra are grouped in subsets (for facilitating the comparison between FIV by active and passive touch) in Figures 11, 12, and 13. The same subsets will be discussed for the discrimination results in section 3.5. Even if, in active touch, the contact boundary conditions (e.g. sliding velocity) depends on the participant's movement, and therefore were not always constant during the stroke, the qualitative behaviour of FIV in active (semi-controlled) conditions and in passive (controlled) conditions is in a very good agreement. The amplitude of the FIV spectra increase with the increase of the roughness and the frequency distribution are consistent in both cases. The vibrational energy is recovered in the same frequency range, with a large band profile. Moreover, for FIV measured from both passive and active touch, a main frequency peak can be distinguished at about 55 Hz for the coarser textures from S1 to S4 in particular), which is due to the fingerprints width of the reference participant for a sliding velocity of 30 mm/s, in agreement with previous results [8,13,23] for coarse textures.

This overall agreement is of main relevance because it allows using active touch, which is the natural way of surface exploration, to measure and mimic the FIV signals.

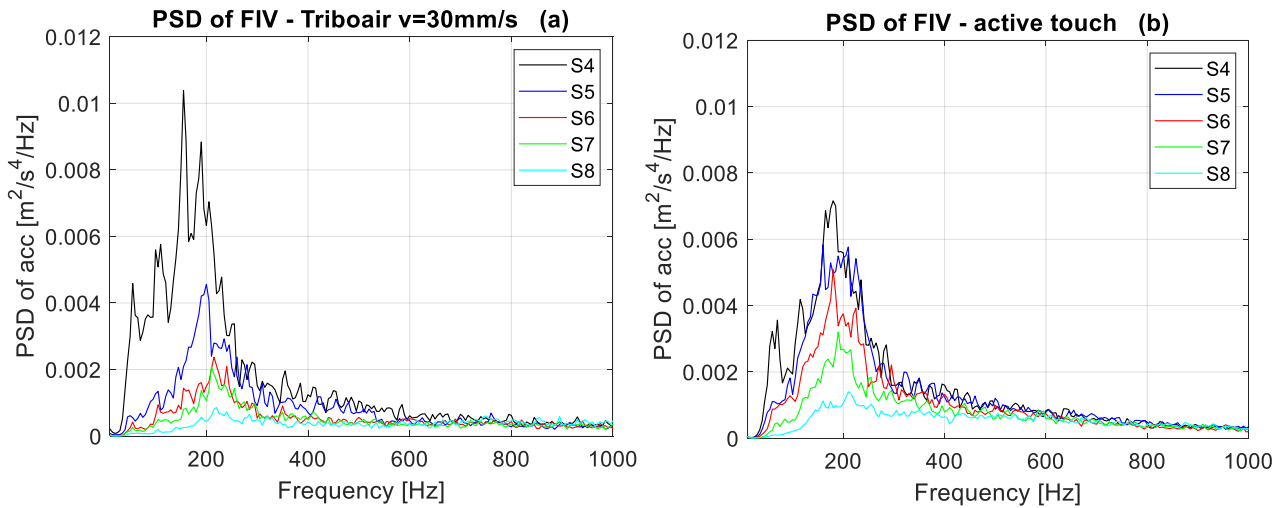


Figure 11: Comparison between FIV spectra by passive touch (a) and active touch (b), for 4 test samples, from S4 to S8 (for the same reference participant).

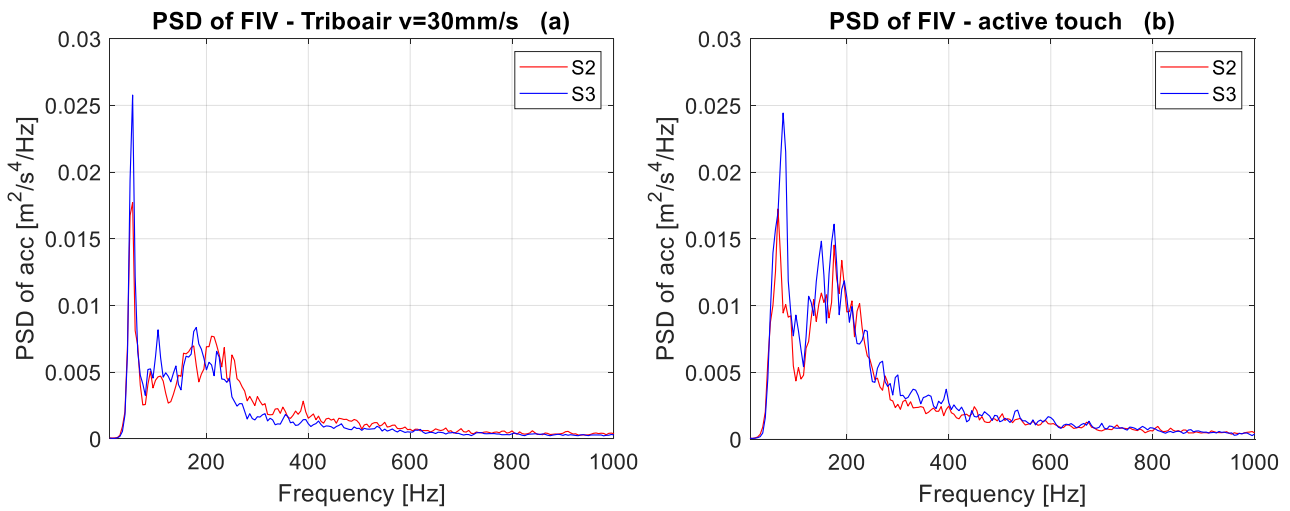


Figure 12: Comparison between FIV spectra by passive touch (a) and active touch (b), for the samples S2 and S3 (for the same reference participant).

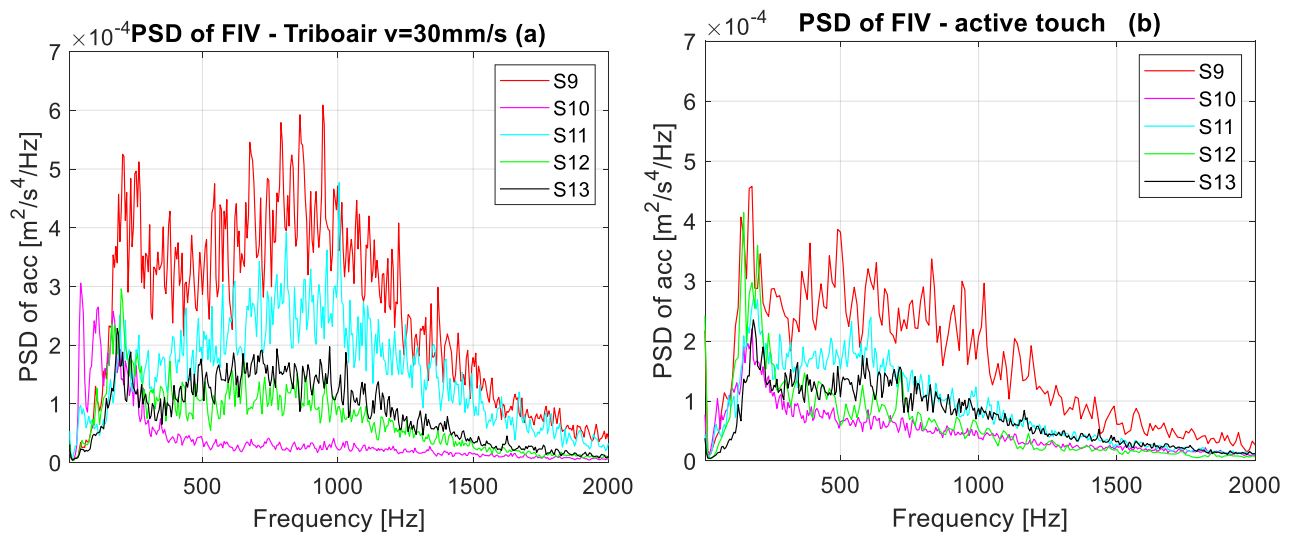


Figure 13: Comparison between FIV spectra by passive touch (a) and active touch (b), for 5 test samples, from S9 to S13 (for the same reference participant).

### 3.4. Discrimination campaigns on real and simulated surfaces

For each of the 3 discrimination tasks, described in section 2.6, the results related to the 10 volunteers have been integrated. The results have been represented and analysed by means of association matrices, built as follows. On the horizontal plane of the association 3D matrix, the abscissa shows the tested samples, and the ordinate reports the answers declared by the participants. This means that the correct associations of the samples are localized on the principal diagonal of the matrix, while the associations out from the diagonal represent the discrimination errors. The vertical axis shows the percentage of each association of samples. The percentage of association was computed as the number of times each association appeared in the whole campaign, divided by the number of times each sample was presented into the whole campaign, multiplied by 100 to express it in percentage.

#### TASK 1

Figure 14a shows the results of the discrimination task 1. In this task, the volunteers dealt with the discrimination of the entire set of 14 samples (real surfaces). High percentage of association are localized on the main diagonal of the matrix, testifying a good performance of the participants to identify the sequence of the explored textures. On the other hand, discrimination errors interested in particular the samples S2 and S3, which have been often confused. As well, discrimination errors occurred for the group of samples from S9 to S13. The “no texture” sample was always correctly positioned in the sequence by all the participants.

#### TASK 2

Figure 14b shows the results of the task 2 of the discrimination campaign. The task was related to the discrimination of the real surface samples, divided into sets, each constituted by 3 samples. The results related to all the sets are reported in the matrix. High percentages of association are localized on the main diagonal of the matrix, testifying an overall good performance of the participants to discriminate the real samples. Some discrimination errors interested again the samples S2 and S3, and most of the errors were registered for the group of samples from S9 to S13, confirming the results obtained for the preliminary task 1.

#### TASK 3

Figure 14c shows the results of the discrimination task 3, related to the simulated textures (reproduced FIV), by the PIEZOTACT device. High percentage of association are localized on the main diagonal of the matrix, testifying a good performance of the participants to discriminate the mimicked textures by the device, thanks to the reproduced FIV stimuli. Again, some discrimination errors are related to the samples S2 and S3, confused with each other, while most of the errors were registered between samples from S9 to S13.

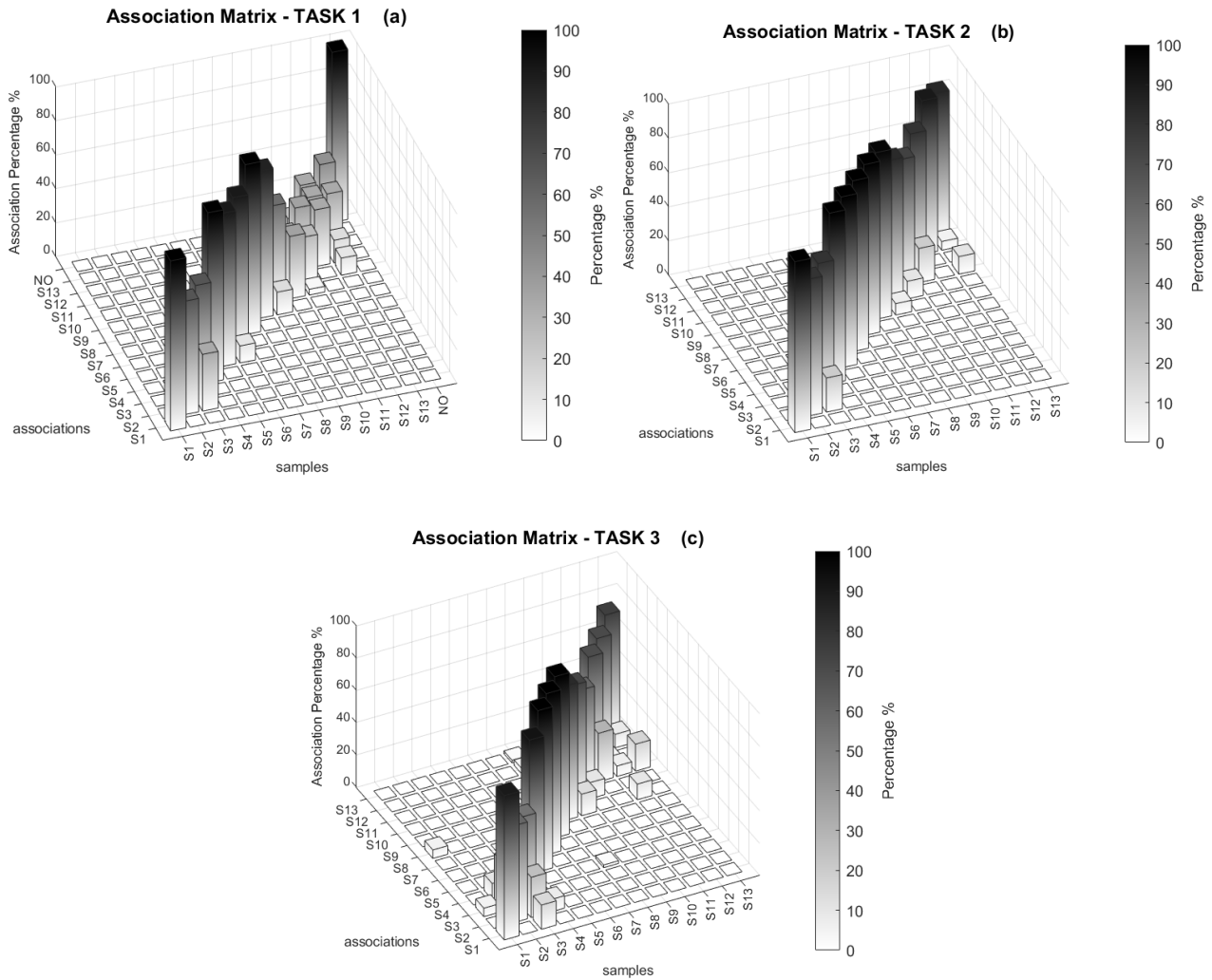


Figure 14: Results of discrimination campaign: results of the preliminary TASK 1 (a) on real surfaces; results of TASK 2 (b) on subsets of real textures; results of TASK 3 (c) on the simulated textures by the PIEZOTACT.

The resulting matrices have been compared in Figure 15, highlighting the areas of the matrices where the discrimination errors were localized. The first task was related to the ordering of the entire sequence of 14 isotropic samples (left), the second task to the discrimination of the real isotropic samples (center), arbitrary divided into sets (each constituted by 3 samples), and the third tasks concerned the simulated surfaces (right), mimicking the FIV by the PIEZOTACT device. Figure 15 highlights that there is a clear agreement between the results of the 3 discrimination tasks. The overall discrimination task showed good results for all the tasks, either with real or simulated surfaces. In all the 3 tasks the main discrimination errors are localized into the same areas of the matrices. In particular, the samples S2 and S3 have been confused during all the 3 tasks, both with real and simulated textures. Moreover, the group of samples, from S9 to S13, underwent to highest percentages of discrimination errors in the all the 3 tasks. The group of samples, from S4 to S8, have always been correctly discriminated in the 3 tasks.

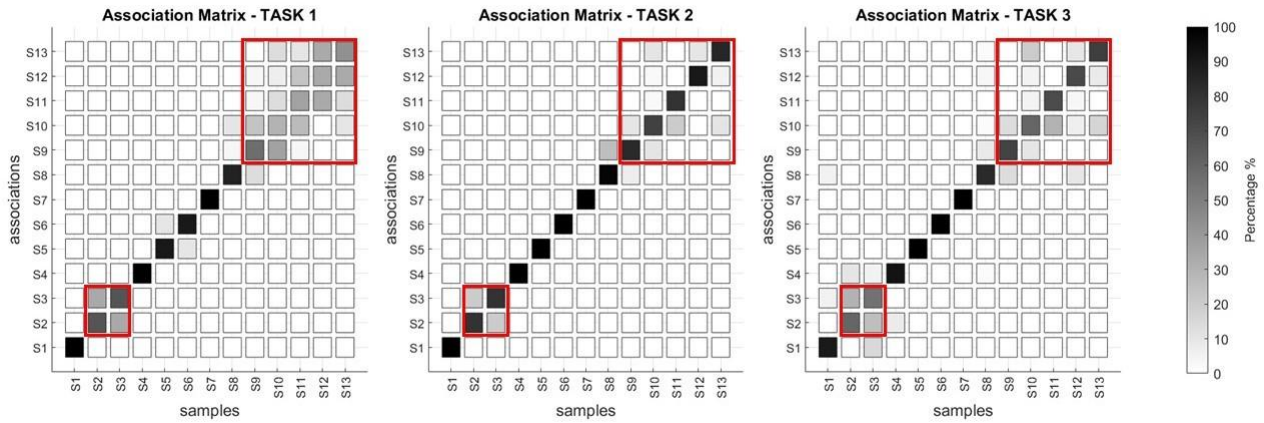


Figure 15: Comparison between the matrices associated to the 3 tasks constituting the discrimination campaign. In all the matrices, the group of samples that have been confused the most have been highlighted.

### 3.5. Overall discussion: discrimination of isotropic textures by FIV

The agreement between the results of the real textures (task 1 and 2) and of the discrimination of the mimicked FIV by the PIEZOTACT device (task 3) testifies the good rendering performance of the PIEZOTACT device and the proposed rendering methodology. In fact, while touch is a very complex sense, which involves many stimuli (vibrations, contact stresses, friction, temperature, humidity, etc.), the PIEZOTACT device and the proposed methodology allowed the rendering of textures, decoupling the FIV stimuli, measured by the accelerometer at the fingernail during the surface exploration, by the other stimuli involved into the overall tactile perception.

The results obtained by the discrimination tasks, with the excellent agreement in discriminating real and simulated surfaces (by only FIV), allows thus to infer the main role played by the FIV stimuli in the perception and discrimination of textures.

Furthermore, the correlation between the FIV spectra and the results of the entire discrimination campaign (composed by the 3 tasks) is here discussed. Figures 12 and 13 show the FIV spectra associated to the groups of samples confused into the entire discrimination campaign, for both real and simulated textures, while Figure 11 shows an always correctly discriminated group of samples. The following observations can be then highlighted:

- The samples S2 and S3, which have been often confused in all the 3 tasks, show FIV with very similar amplitude and frequency distribution (Fig. 12).
- Similarly, the group of samples from S9 to S13 undergone to confusion in the entire campaign. The 10 participants had difficult to discriminate this group of samples both in the case of the real samples and in the one related to the mimicked FIV. During the Task 1, related to the entire sequence of 14 real samples, the percentages of error were very high for the considered group of samples. Again, the FIV spectra, associated to these samples (Fig. 13), show similar amplitudes, and inversions of amplitudes with respect to the surface roughness.
- The frequency distribution shows, for this group of smoother samples (from S9 to S13), a large band at higher frequencies. On the contrary, the sample S10 presents a spectrum at lower frequencies, probably due to local stick-slip phenomena on the surface, that could confuse the participants.
- On the contrary, by observing the FIV spectra related to the samples from S4 to S8 (Fig. 11), which have been always correctly discriminated during the 3 tasks, it turns out that they show clearly different amplitudes of the FIV spectra.

Figure 16 shows the sample roughness (Ra) compared with the RMS of the FIV measured during passive touch (controlled velocity of 30mm/s) for a reference participant.

The roughness is decreasing from S1 to S14.

On another hand, when considering the FIV amplitude, from sample S1 to sample S9, the RMS decreases with the roughness, while, from sample S10 to sample S13, the trend of the RMS of the FIV presents inversions with respects to the roughness. When considering the results from the discrimination campaigns, the following considerations can be made:

- Samples from S1 to S9 have been generally well discriminated, with some exceptions:
  - The samples S2 and S3, which have been confused in the entire discrimination campaign, present very similar RMS of induced vibrations, although they present clearly different Ra.
  - As well, the samples S8 and S9 present a very similar RMS but a different Ra and, in some cases, the samples have been confused in the discrimination campaigns.
- On the contrary, the samples from S10 to S13 underwent the highest percentage of errors in the entire discrimination campaign. In accordance, their RMS present similarities and inversions with to respect to the sample roughness.
- Moreover, samples S7 and S8 present similar values of Ra, but they have been always well discriminated in the entire campaign. In accordance, the associated RMS of FIV and the FIV spectra (Figure 11) are clearly different.

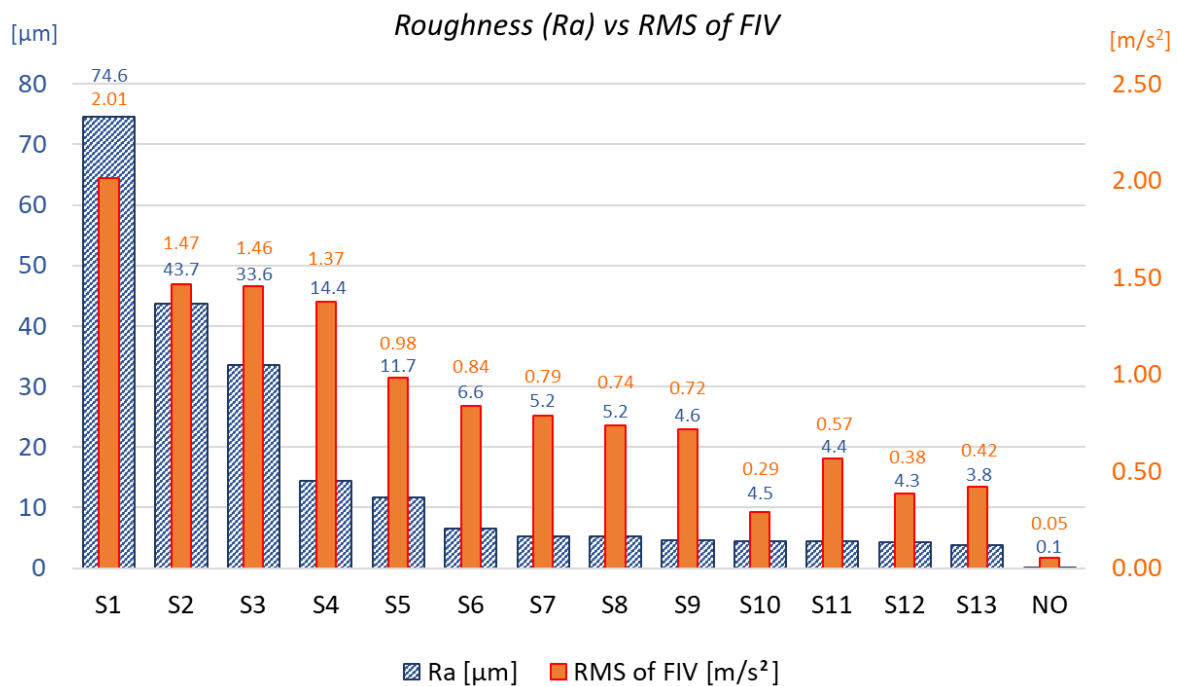


Figure 16: Ra roughness vs RMS of FIV (acceleration) for passive touch of the 14 isotropic samples for a reference participant.

Summarising, the trend of the FIV (RMS and spectral distribution) agrees with the results obtained in the discrimination campaign on real and simulated textures. The discrimination errors occurred each time the FIV amplitude were similar or reversed, with respect to the roughness.

The FIV, and in particular the RMS of FIV amplitude, were then able to explain the perception and discrimination of the textures under examination, while an average roughness parameter did not prove to

be a good indicator to explain the perception and discrimination. It should be kept in mind that the mechanical signal directly received by the mechanoreceptor is the skin transient deformation (vibrations) and not the topography.

From Figure 16 it can be noticed as well that the samples with higher difficulty to be discriminated are the ones under a certain level of FIV amplitude (about  $0.7 \text{ m/s}^2$  in Figure 16). In future works it would be interesting to investigate if there is a sensitivity threshold below which the vibrations, induced by the tactile exploration of the surface, are too low to allow the clear discrimination of textures. For the reference subject, presented in Figure 16, this threshold could be identified by an RMS value around  $0.7 \text{ m/s}^2$ .

The results of the presented discrimination campaign on isotropic randomly rough samples agree with the results obtained for periodic textures in [9]. In both cases, for periodic and random surfaces, the participants were able to associate the simulated textures (reproduced FIV) by the PIEZOTACT device to the real ones, with very good percentages of success. Moreover, in both the studies (the present study and the one reported in [9]), it was possible to well correlate the results of the discrimination campaign with the FIV spectra, despite the discrimination of periodic textures turned out to be more driven by the FIV frequency distribution [9,13], while the isotropic textures resulted to be discriminated by the FIV amplitude, rather than their distribution in frequency.

## 4. Conclusions

Isotropic randomly rough surface samples have been manufactured starting from glasspaper ranging between very coarse grain sizes to very fine ones. The mechanical stimuli, the Friction-Induced Vibrations, associated to the exploration of the random surfaces have been measured and analysed by active and passive touch. The measured FIV have been then reproduced by means of a vibrotactile device, in order to render the surface textures. Discrimination campaigns have been performed, both with the real samples and the simulated textures by the device. The results of the discrimination campaigns showed, in general, a good performance of the subjects to discriminate both real and simulated (by FIV) textures, with an excellent agreement between the results obtained by the mimicked and the real textures. In fact, the discrimination errors interested the same groups of samples in all the campaigns. These errors have been clearly associated to the features of the FIV spectra, i.e. the mostly confused samples showed similar FIV amplitude or amplitude inversions, with respect to the sample roughness. Samples that were always correctly discriminated showed instead FIV spectra with clearly different amplitude, without amplitude inversions with respect to the roughness. While  $R_a$  roughness did not prove to be a good indicator with, respect to the tactile discrimination of the examined textures, spectral analyses on the topographies could be conducted to investigate whether it is possible to find topographic features that correlate with the perception and discrimination of isotropic textures.

Moreover, from the analysis of the FIV spectra, it turned out that the key feature in the discrimination of the isotropic samples is the FIV amplitude, contrarily with respect to previous results found in periodic textures [13], where the FIV frequency distribution prevails. All the presented analyses show the main role played by the FIV in the discrimination of textures. Future works will be addressed to the identification of a possible threshold effect on the amplitude of the stimuli, under which the textures are no more discriminated by the subjects.

## Acknowledgments

The authors thank ARKEMA-Piezotech for providing the used piezoelectric electro-active polymers for this study.

This work was supported by the project CONTACT (ANR 2020-CE28-0010-03), funded by the french “Agence Nationale de la Recherche” (ANR).

## References

- [1] R. S. Johansson and Å. B. Vallbo, “Tactile sensory coding in the glabrous skin of the human hand,” *Trends in Neurosciences*, vol. 6, pp. 27-32, 1983.
- [2] K. O. Johnson, “The roles and functions of cutaneous mechanoreceptors,” *Current opinion in neurobiology*, vol. 11, p. 455–461, 2001.
- [3] I. Cesini, J. D. Ndengue, E. Chatelet, J. Faucheu and F. Massi, “Correlation between friction-induced vibrations and tactile perception during exploration tasks of isotropic and periodic textures,” *Tribology International*, vol. 120, p. 330–339, 2018.
- [4] J. Dacleu Ndengue, I. Cesini, J. Faucheu, E. Chatelet, H. Zahouani, D. Delafosse and F. Massi, “Tactile Perception and Friction-Induced Vibrations: Discrimination of Similarly Patterned Wood-Like Surfaces,” *IEEE Transactions on Haptics*, vol. 10, pp. 409-417, 2017.
- [5] B. Delhaye, V. Hayward, P. Lefèvre and J.-L. Thonnard, “Texture-induced vibrations in the forearm during tactile exploration,” *Frontiers in Behavioral Neuroscience*, vol. 6, 2012.
- [6] M. Di Bartolomeo, F. Morelli, D. Tonazzi, F. Massi and Y. Berthier, “On the role of friction induced vibrations in tactile perception,” *Proceedings of ISMA 2016 - International Conference on Noise and Vibration Engineering and USD2016 - International Conference on Uncertainty in Structural Dynamics*, pp. 3099-3110, 2016.
- [7] R. Fagiani, F. Massi, E. Chatelet, Y. Berthier and A. Sestieri, “Experimental analysis of friction-induced vibrations at the finger contact surface,” *Proceedings of the Institution of Mechanical Engineers, Part J: Journal of Engineering Tribology*, vol. 224, pp. 1027-1035, 2010.
- [8] R. Fagiani, F. Massi, E. Chatelet, Y. Berthier and A. Akay, “Tactile perception by friction induced vibrations,” *Tribology International*, vol. 44, p. 1100–1110, 2011.
- [9] L. Felicetti, E. Chatelet, A. Latour, P.-H. Cornuault and F. Massi, “Tactile rendering of textures by an Electro-Active Polymer piezoelectric device: mimicking Friction-Induced Vibrations,” *Biotribology*, vol. 31, p. 100211, 2022.
- [10] C. M. Greenspon, K. R. McLellan, J. D. Lieber and S. J. Bensmaia, “Effect of scanning speed on texture-elicited vibrations,” *Journal of The Royal Society Interface*, vol. 17, p. 20190892, 2020.
- [11] J. Hu, X. Zhang, X. Yang, R. Jiang, X. Ding and R. Wang, “Analysis of fingertip/fabric friction-induced vibration signals toward vibrotactile rendering,” *The Journal of The Textile Institute*, vol. 107, p. 967–975, 2016.

- [12] R. Jiang, J. Hu, X. Yang and X. Ding, "Analysis of fingertip/textile friction-induced vibration by time-frequency method," *Fibers and Polymers*, vol. 17, p. 630–636, 2016.
- [13] V. Massimiani, B. Weiland, E. Chatelet, P.-H. Cornuault, J. Faucheu and F. Massi, "The role of mechanical stimuli on hedonistic and topographical discrimination of textures," *Tribology International*, vol. 143, p. 106082, 2020.
- [14] R. Sahli, A. Prot, A. Wang, M. H. Müser, M. Piovarči, P. Didyk and R. Bennewitz, "Tactile perception of randomly rough surfaces," *Scientific reports*, vol. 10, p. 1–12, 2020.
- [15] X. Zhou, J. L. Mo, Y. Y. Li, Z. Y. Xiang, D. Yang, M. A. Masen and Z. M. Jin, "Effect of finger sliding direction on tactile perception, friction and dynamics," *Tribology Letters*, vol. 68, p. 1–13, 2020.
- [16] S. J. Lederman, "The perception of surface roughness by active and passive touch," *Bulletin of the Psychonomic Society*, vol. 18, p. 253–255, 1981.
- [17] L. Felicetti, E. Chatelet, A. Latour and F. Massi, "Analysis and mimicking of contact vibrations, induced by touching isotropic surface textures," in *Proceedings of ISMA2022 - International Conference on Noise and Vibration Engineering, September 12-14, 2022*, Leuven, Belgium, 2022.
- [18] İ. M. Koç and C. Aksu, "Tactile sensing of constructional differences in fabrics with a polymeric finger tip," *Tribology International*, vol. 59, pp. 339-349, 2013.
- [19] X. Zhou, J. L. Mo, Y. Y. Li, J. Y. Xu, X. Zhang, S. Cai and Z. M. Jin, "Correlation between tactile perception and tribological and dynamical properties for human finger under different sliding speeds," *Tribology International*, vol. 123, pp. 286-295, 2018.
- [20] S. J. Bensmaïa and M. Hollins, "The vibrations of texture," *Somatosensory & motor research*, vol. 20, p. 33–43, 2003.
- [21] S. Bensmaïa and M. Hollins, "Pacianian representations of fine surface texture," *Perception & psychophysics*, vol. 67, p. 842–854, 2005.
- [22] S. J. Lederman and R. L. Klatzky, "Haptic perception: A tutorial," *Attention, Perception, & Psychophysics*, vol. 71, p. 1439–1459, 2009.
- [23] R. Fagiani, F. Massi, E. Chatelet, J. P. Costes and Y. Berthier, "Contact of a finger on rigid surfaces and textiles: Friction coefficient and induced vibrations," *Tribology Letters*, vol. 48, p. 145–158, 2012.
- [24] M. Hollins and S. R. Risner, "Evidence for the duplex theory of tactile texture perception," *Perception & psychophysics*, vol. 62, p. 695–705, 2000.
- [25] J. Scheibert, S. Leurent, A. Prevost and G. Debrégeas, "The role of fingerprints in the coding of tactile information probed with a biomimetic sensor," *Science*, vol. 323, p. 1503–1506, 2009.
- [26] A. Prevost, J. Scheibert and G. Debrégeas, "Effect of fingerprints orientation on skin vibrations during tactile exploration of textured surfaces," *Communicative & Integrative Biology*, vol. 2, pp. 422-424, 2009.
- [27] G. Lacerra, M. Di Bartolomeo, S. Milana, L. Baillet, E. Chatelet and F. Massi, "Validation of a new frictional law for simulating friction-induced vibrations of rough surfaces," *Tribology International*, vol. 121, p. 468–480, 2018.

- [28] M.-A. Bueno, B. Lemaire-Semail, M. Amberg and F. Giraud, "A simulation from a tactile device to render the touch of textile fabrics: a preliminary study on velvet," *Textile Research Journal*, vol. 84, p. 1428–1440, 2014.
- [29] M. Di Bartolomeo, F. Morelli, D. Tonazzi, F. Massi and Y. Berthier, "Investigation of the role of contact-induced vibrations in tactile discrimination of textures," *Mechanics & Industry*, vol. 18, p. 404, 2017.
- [30] C. Basdogan, F. Giraud, V. Levesque and S. Choi, "A Review of Surface Haptics: Enabling Tactile Effects on Touch Surfaces," *IEEE Transactions on Haptics*, vol. 13, pp. 450-470, 2020.
- [31] S. Choi and K. J. Kuchenbecker, "Vibrotactile Display: Perception, Technology, and Applications," *Proceedings of the IEEE*, vol. 101, pp. 2093-2104, 2013.
- [32] L. A. Jones and N. B. Sarter, "Tactile Displays: Guidance for Their Design and Application," *Human Factors*, vol. 50, pp. 90-111, 2008.
- [33] R. H. Osgouei, "Electrostatic Friction Displays to Enhance Touchscreen Experience," in *Modern Applications of Electrostatics and Dielectrics*, D. Xiao and K. Sankaran, Eds., Rijeka, IntechOpen, 2020.
- [34] A. Costes, F. Danieau, F. Argelaguet, P. Guillotel and A. Lécuyer, "Towards Haptic Images: A Survey on Touchscreen-Based Surface Haptics," *IEEE Transactions on Haptics*, vol. 13, pp. 530-541, 2020.
- [35] H. Culbertson, J. Unwin and K. J. Kuchenbecker, "Modeling and rendering realistic textures from unconstrained tool-surface interactions," *IEEE transactions on haptics*, vol. 7, p. 381–393, 2014.
- [36] J. M. Romano and K. J. Kuchenbecker, "Creating Realistic Virtual Textures from Contact Acceleration Data," *IEEE Transactions on Haptics*, vol. 5, pp. 109-119, 2012.
- [37] P. Strohmeier and K. Hornbæk, "Generating haptic textures with a vibrotactile actuator," in *Proceedings of the 2017 CHI Conference on Human Factors in Computing Systems*, p. 4994–5005, 2017.
- [38] S. Wu, X. Sun, Q. Wang and J. Chen, "Tactile modeling and rendering image-textures based on electrovibration," *The Visual Computer*, vol. 33, p. 637–646, 2017.
- [39] R. H. Osgouei, J. R. Kim and S. Choi, "Data-Driven Texture Modeling and Rendering on Electro-vibration Display," *IEEE Transactions on Haptics*, vol. 13, pp. 298-311, 2020.
- [40] T. Vodlak, Z. Vidrih, E. Vezzoli, B. Lemaire-Semail and D. Peric, "Multi-physics modelling and experimental validation of electrovibration based haptic devices," *Biotribology*, vol. 8, pp. 12-25, 2016.
- [41] J. Jiao, Y. Zhang, D. Wang, Y. Visell, D. Cao, X. Guo and X. Sun, "Data-driven rendering of fabric textures on electrostatic tactile displays," in *2018 IEEE Haptics Symposium (HAPTICS)*, p. 169-174, 2018.
- [42] R. H. Osgouei, S. Shin, J. R. Kim and S. Choi, "An inverse neural network model for data-driven texture rendering on electrovibration display," in *2018 IEEE Haptics Symposium (HAPTICS)*, p. 270-277, 2018.
- [43] B. Camillieri, M.-A. Bueno, M. Fabre, B. Juan, B. Lemaire-Semail and L. Mouchnino, "From finger friction and induced vibrations to brain activation: Tactile comparison between real and virtual textile fabrics," *Tribology International*, vol. 126, p. 283–296, 2018.

- [44] M. Wiertlewski, D. Leonardis, D. J. Meyer, M. A. Peshkin and J. E. Colgate, "A High-Fidelity Surface-Haptic Device for Texture Rendering on Bare Finger," in *Haptics: Neuroscience, Devices, Modeling, and Applications*, vol. 8619, Berlin, 2014.
- [45] M. Wiertlewski, R. F. Friesen and J. E. Colgate, "Partial squeeze film levitation modulates fingertip friction," *Proceedings of the national academy of sciences*, vol. 113, p. 9210–9215, 2016.
- [46] G. Liu, C. Zhang and X. Sun, "Tri-Modal Tactile Display and Its Application Into Tactile Perception of Visualized Surfaces," *IEEE Transactions on Haptics*, vol. PP, pp. 1-1, March 2020.
- [47] H. Culbertson and K. J. Kuchenbecker, "Importance of Matching Physical Friction, Hardness, and Texture in Creating Realistic Haptic Virtual Surfaces," *IEEE Transactions on Haptics*, vol. 10, p. 63–74, January 2017.
- [48] A. Abdulali and S. Jeon, "Data-Driven Rendering of Anisotropic Haptic Textures," in *Haptic Interaction*, p. 401–407, Singapore, 2018.
- [49] A. M. Okamura, J. T. Dennerlein and R. D. Howe, "Vibration feedback models for virtual environments," in *Proceedings. 1998 IEEE International Conference on Robotics and Automation (Cat. No.98CH36146)*, 1998.
- [50] S. Shin, R. H. Osgouei, K.-D. Kim and S. Choi, "Data-driven modeling of isotropic haptic textures using frequency-decomposed neural networks," in *2015 IEEE World Haptics Conference (WHC)*, p. 131-138, 2015.
- [51] J. Jiao, Y. Zhang, D. Wang, X. Guo and X. Sun, "HapTex: A Database of Fabric Textures for Surface Tactile Display," in *2019 IEEE World Haptics Conference (WHC)*, 2019.
- [52] H. Culbertson, J. J. López Delgado and K. J. Kuchenbecker, "One hundred data-driven haptic texture models and open-source methods for rendering on 3D objects," in *IEEE Haptics Symposium (HAPTICS)*, p. 319-325, 2014.
- [53] M. Strese, J.-Y. Lee, C. Schuwerk, Q. Han, H.-G. Kim and E. Steinbach, "A haptic texture database for tool-mediated texture recognition and classification," in *IEEE International Symposium on Haptic, Audio and Visual Environments and Games (HAVE) Proceedings*, p. 118-123, 2014.
- [54] C. Frisson, J. Decaudin, T. Pietrzak, A. Ng, P. Poncet, F. Casset, A. Latour and S. A. Brewster, "Designing Vibrotactile Widgets with Printed Actuators and Sensors," in *Adjunct Publication of the 30th Annual ACM Symposium on User Interface Software and Technology*, p. 11–13, New York, NY, USA, 2017.
- [55] N. Godard, L. Alliol, A. Latour, S. Glinsek, M. Gérard, J. Polesel, F. D. D. Santos and E. Defay, "1-mW Vibration Energy Harvester Based on a Cantilever with Printed Polymer Multilayers," *Cell Reports Physical Science*, vol. 1, p. 100068, 2020.
- [56] P. Poncet, F. Casset, A. Latour, F. Domingues Dos Santos, S. Pawlak, R. Gwoziecki and S. Fanget, "Design and realization of electroactive polymer actuators for transparent and flexible haptic feedback interfaces," in *17th International Conference on Thermal, Mechanical and Multi-Physics Simulation and Experiments in Microelectronics and Microsystems (EuroSimE)*, p. 1-5, 2016.

- [57] P. Poncet, F. Casset, A. Latour, F. Domingues Dos Santos, S. Pawlak, R. Gwoziecki, A. Devos, P. Emery and S. Fanget, "Static and dynamic studies of electro-active polymer actuators and integration in a demonstrator," in *Actuators*, 2017.
- [58] İ. M. Koç and E. Akça, "Design of a piezoelectric based tactile sensor with bio-inspired micro/nano-pillars," *Tribology International*, vol. 59, pp. 321-331, 2013.
- [59] A. Lazzari, D. Tonazzi, J. Brunetti, A. Saulot and F. Massi, "Contact instability identification by phase shift on C/C friction materials," *Mechanical Systems and Signal Processing*, vol. 171, p. 108902, 2022.
- [60] M. D. Bartolomeo, A. Lazzari, M. Stender, Y. Berthier, A. Saulot and F. Massi, "Experimental observation of thermally-driven frictional instabilities on C/C materials," *Tribology International*, vol. 154, p. 106724, 2021.
- [61] S. J. Lederman and M. M. Taylor, "Fingertip force, surface geometry, and the perception of roughness by active touch," *Perception & psychophysics*, vol. 12, p. 401-408, 1972.